Biol. Cybern. 79, 301–308 (1998)

Biological Cybernetics

Statistical model of the hippocampal CA3 region
I. The single-cell module: bursting model of the pyramidal cell

T. Grőbler, G. Barna, P. Érdi

Department of Biophysics, KFKI Research Institute for Particle and Nuclear Physics of the Hungarian Academy of Sciences, P.O. Box 49, H-1525 Budapest, Hungary

Received: 29 August 1997 / Accepted in revised form: 17 July 1998

Abstract. A model with intermediate complexity is introduced to reproduce the basic firing modes of the CA3 pyramidal cell. Our model consists of a single compartment, has two variables (membrane potential and internal calcium concentration), and involves two separate stages for interspike mechanisms and firing. Interspike dynamics is governed by voltage- and calcium-dependent ionic channels but no channel kinetics are provided. This model is suitable to be included in our statistical population model (Part II, following paper). Bifurcation analysis reveals that interspike dynamics rather than sodium firing has the dominant role in the control of bursting/nonbursting behavior.

1 Introduction

The brain is a prototype of hierarchical structures, and its dynamics can and should be studied at different levels of organization (Arbib et al. 1997). Structure-based bottom-up modeling has two extreme alternatives, namely the multi-compartmental technique and the simulation of networks composed of simple elements. There is an obvious trade-off between these two modeling strategies. The first method is appropriate for describing the activity patterns of single cells, small networks based on data on detailed morphology, and the kinetics of voltage- and calcium-dependent ion channels. The second strategy offers a computationally efficient method for simulating large networks of neurons where the details of single-cell properties are neglected.

The behavior of large networks of neurons may, on the other hand, be studied by statistical population theories. Just as collective phenomena emerging in physical systems of a large number of elementary components are treated by statistical mechanics, so have statistical dynamics theories of neural populations been established (Beurle 1956; Griffith 1963; Seelen 1968; Wilson and Cowan 1973; Amari 1974; Ventriglia 1974; Ingber 1982; Peretto 1984; Clark et al. 1985; Ventriglia 1988; Peresto 1992; Ventriglia 1994). Statistical theories work with distributions and averaged quantities. Neuronal population theories established up to this time have used oversimplified single-cell models. One important example for the oversimplification of such models is their lack of ability to generate burst. As is well known, cortical and hippocampal pyramidal cells may work in burst mode. It was suggested (Lisman 1997) that bursts (and not unreliable action potentials) may serve as a unit of neural information.

Our aim is to develop a general theory of neuronal populations, and to apply it to the simulation of large-scale hippocampal activity (Grőbler and Barna 1996; Érdi et al., 1997; Gröbler and Barna 1997). To achieve this goal first (Part I), we establish a single-compartmental bursting model of pyramidal cells exhibiting intermediate complexity. We show that the model is capable of reproducing the basic firing modes of the pyramidal cells demonstrated both experimentally and by detailed multicompartmental modeling (Traub and Miles 1991; Traub et al. 1991, 1992).

Then (Part II) a statistical theory of interacting neural fields, motivated by Ventriglia's kinetic theory (Ventriglia 1974, 1988, 1994) is established and our single-cell module is incorporated in the population framework. With the population model we simulate the normal and epileptic activities of the CA3 region of hippocampal slices.

In this paper we construct a single-cell model which is intended to be sufficiently complex to describe the gross behavior, i.e. basic firing patterns, bifurcation schemes, and current–frequency relationships, of the pyramidal cell, and sufficiently simple to be the building block of a computationally tractable neural population model.

The existing realistic single-cell models are based on Hodgkin–Huxley-type equations (Hodgkin and Huxley 1952) by taking into account the membrane currents underlying the generation and propagation of action potentials. Neural simulation systems such as NEURON (Hines 1984, 1993) and GENESIS (Wilson and Bower

Correspondence to: P. Érdi (e-mail: erdi@rmki.kfki.hu)

1989; Bower and Beeman 1995) have been constructed to simplify the efficient simulation of branched neurons.

Pinsky and Rinzel (1994) presented a two-compartment model of a CA3 pyramidal cell as a reduction of Traub's (Traub et al. 1991) 19-compartment model. They wrote (p. 40):

> 'We view Traub's CA3 system as a computational analog of an experimental preparation for which all components are known and for which a substantial amount of behavioral repertoire has been described. We ask, what is a minimal biophysical/mathematical description which can account semi-quantitatively for the [...] dynamical features of this model system. Just as the Traub model represents the biological CA3 system in an oversimplified but valuable way, we find that this description can be further idealized while still achieving some accountability. Moreover, by reducing the model's complexity and computational demand we seek to identify the dominant qualitative mechanisms for certain aspects of the system's behavior.'

Our aim is to construct an even simpler model with the same purpose. The model we present here is a *single-compartment* description, and the channel gating kinetics are omitted. Still, we would like to show that the basic dynamical properties of pyramidal cells are preserved.

The crucial assumption behind a single-compartment model is that the whole cell can be characterized by a single membrane potential. The original Hodgkin–Huxley system and even its generalizations have been the subject of approximative reduction procedures for obtaining two-dimensional systems (e.g. FitzHugh 1961; Nagumo et al. 1962; Hindmarsh and Rose 1982; Kepler et al. 1992). One advantage of two-dimensional systems is that they can easily be visualized and analyzed by applying phase-space techniques (Ermentrout 1995).

Bursting patterns are generally the results of the interplay of slow and fast subsytems. Hindmarsh and Rose (1984) presented a model of neuronal bursting by using three variables. A formal classification of bursting mechanisms was given by Rinzel (1987). The models contain an equation for the temporal change of the membrane potential, and a set of kinetic equations for the gating variables.

Considering our approach to the single-cell dynamics from the point of view of conductance-based models, we neglect the sodium spike generating mechanism, since the form of the action potential does not bear too much information. Therefore spike generation is described by some computationally cheap algorithm.

Models with intermediate complexity can be derived not only by reducing the realistic model framework but also by adding realistic elements to the abstract models. Dynamic thresholds (Horn and Usher 1989) and the simplified description of the ionic mechanisms by a generalized activation function (Cartling 1995) were offered. Our model explicitly describes the interspike dynamics by using the membrane potential and the calcium concentration as variables, and specifes the firing probability.

2 The model

The single-cell model presented here is a hippocampal CA3 pyramidal cell model. With some reduction, however, a very simple inhibitory cell model can also be obtained (Sect. 2.4) which will be used in the population model (Part II).

2.1 General properties

The model consists of a *single compartment* and thus has no extension in space. The effect of synaptic actions occurring at distant dendritic locations appears as temporally elongated post-synaptic currents as detected by the soma. The axon is only taken into account in the population model (Part II).

One of the most important dynamic properties of pyramidal cells is their capability of intrinsic bursting. It has long been recognized (Wong and Prince 1978) that calcium, and voltage-dependent calcium channels in particular, play a critical role in the generation and maintenance of the bursts. The termination of bursts is, on the other hand, a result of the action of calcium concentration-dependent potassium channels. Thus, our single-compartment model of the pyramidal cell, aiming at the minimal description, contains *two variables*: membrane potential and internal calcium concentration. The interspike behavior of the model is governed by three types of ionic currents: K^+_{DR}, Ca^{2+}, and K^+_{Ca} currents, and a leakage current.

The timing of individual sodium spikes is controlled by the input and different ionic channels. The exact shape of a single spike, however, plays little role in this mechanism. Therefore, in our description the sodium spike is replaced by a simple *refractory period* during which the synaptic actions are performed. The voltage dependent *firing probability* includes the effect of the sodium current as well. After 'firing' a calcium concentration-dependent *return potential* is restored and the intracellular *calcium concentration is increased*.

In summary, pyramidal cells are characterized by: single-compartment multi-channel kinetics; separate mechanisms for interspike activity and firing; two variables: membrane potential (V) and Ca^{2+}-concentration (X); ionic current-controlled interspike behavior and bursting properties; voltage-dependent firing probability.

It is required that our model (1) can reproduce the basic firing modes of pyramidal cells; (2) can be incorporated into the population model (Part II).

Because of the properties of the population model (to be discussed in Part II), the second requirement implies that the factors changing the state (voltage and calcium concentration) of a neuron should *not* depend on past states. (They may depend on the current state or a past event, e.g. synaptic input, that equally effects all states.) Therefore the kinetics of the gating variables of ionic channels are omitted, and all gating variables are replaced with their asymptotic values.

2.2 Interspike dynamics

The equations governing interspike dynamics are the following:

$$-C\frac{dV}{dt} = I_{Ca}(V) + I_K(V) + I_{K[Ca]}(V,X) + I_L(V) + I_{ext} \quad (1)$$

$$\frac{dX}{dt} = -\beta X - BI_{Ca}(V) \quad (2)$$

where C is the membrane capacitance, β is the calcium decay constant, B is a scaling factor between the calcium current and the range of calcium concentration, and the current terms I_{Ca}, $I_{K[Ca]}$, I_K, and I_L are simple functions of V and X. We should note that $I_{K[Ca]}$ is a mixture of different calcium-dependent potassium chanels (e.g. I_C and I_{AHP}). The voltage (and calcium) dependence of the ionic currents and the other parameter values are given in the Appendix.

The initial values (V_0, X_0) for Eqs. (1) and (2) are resting conditions before the first firing, and later are determined by the return values (V_{ret}, X_{ret}) restored after firing (see Sect. 2.3).

A good qualitative picture of the model's interspike behavior can be obtained by the two-dimensional vector field representation of Eqs. (1) and (2) with no external input (Fig. 1A). At each point of this map a vector is shown whose voltage coordinate is the r.h.s. of Eq. (1) at this point, and the calcium coordinate is the r.h.s. of Eq. (2). The direction of such a vector then denotes the direction where the state (V,X) tends to change; the length of the vector denotes the rate of this change. The maximal firing probability Θ and the restored membrane potential as a function of calcium concentration are also shown.

A more conventional way of representing voltage-dependent currents is the current–voltage diagram (Fig. 1B). Since one of the currents is calcium dependent, however, the current–voltage plot is different for different calcium concentrations. Figure 1B shows the current–voltage curves for selected calcium concentration values. Current–voltage diagrams were given by Traub et al. (1991, Fig. 3) for different compartments of their pyramidal cell model. Our diagram shows similarity with their curves for the proximal dendrite since our single-compartment model includes both somatic and dendritic currents.

2.3 Firing

The term 'firing' is used here as referring only to sodium spikes. The bursting property of CA3 pyramidal cells requires a range of membrane potentials where the firing probability is high (sodium channels active) but also the possibility, at higher potentials, of increasing the membrane potential without sodium firing (calcium spike). Thus the firing probability $P(V_1, V_2)$ is determined in the following way:

1. $P(V_1, V_2)$ is the probability that the cell fires while its membrane potential changes from V_1 to V_2.

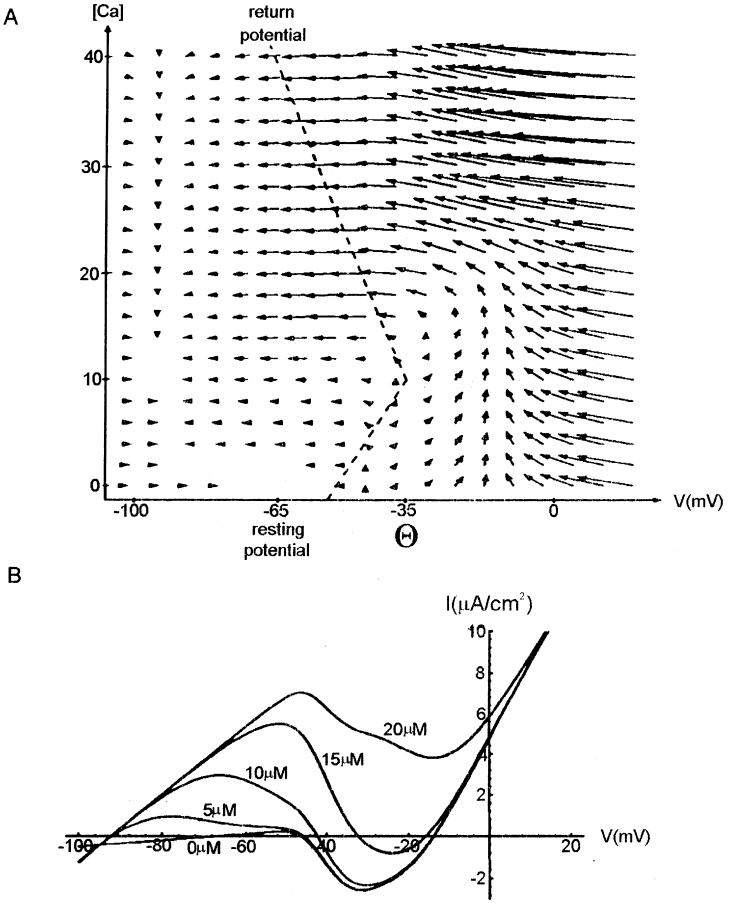

Fig. 1. A Representation of interspike dynamics. *Arrows* represent the magnitude and direction of the change of state at each point. *Dashed line*: the calcium-dependent return potential after firing. **B** Current-voltage diagram of interspike dynamics at different calcium concentrations (cf. Traub et al. 1991; Fig. 3)

2. $P(V_1, V_2)$ is independent of the time to get from V_1 to V_2.
3. Most of the firing occurs around a threshold Θ, i.e. $P(V_1, \infty)$ is close to 1 if $V_1 < \Theta$ but it decreases rapidly if $V_1 > \Theta$.

To fulfill these requirements, the function P is constructed in the Appendix. Its curves for different values of V_1 are shown in Fig. 2.

When the cell has fired, it stays in *refractory state* for a specified time t^{ref}. After this time it *returns* to the stage of interspike dynamics. The $(V_{\text{ret}}, X_{\text{ret}})$ values that are restored when the cell returns from firing are shown as a dashed line in Fig. 1A and are given in the Appendix.

2.4 Inhibitory cells

Inhibitory cells are both anatomically and physiologically heterogeneous (Freund and Buzsáki 1996). Here we neglect the differences between the different types of interneurons and assume that inhibitory cells can be modeled as leaky integrator units, with a single membrane potential variable. This can be obtained by omitting the role of calcium and the voltage-dependent ionic currents from the pyramidal cell model. The interspike behavior then is:

$$C\frac{dV}{dt} = -(I_L(V) + I_{\text{ext}}) \tag{3}$$

The firing of inhibitory cells is deterministic and characterized by a single threshold Θ:

$$P(V_1, V_2) = \begin{cases} 1 & \text{if } V_1 < \Theta \text{ and } V_2 > \Theta \\ 0 & \text{otherwise} \end{cases} \tag{4}$$

After firing the resting potential is restored:

$$V_{\text{ret}} = E_{\text{rest}} \tag{5}$$

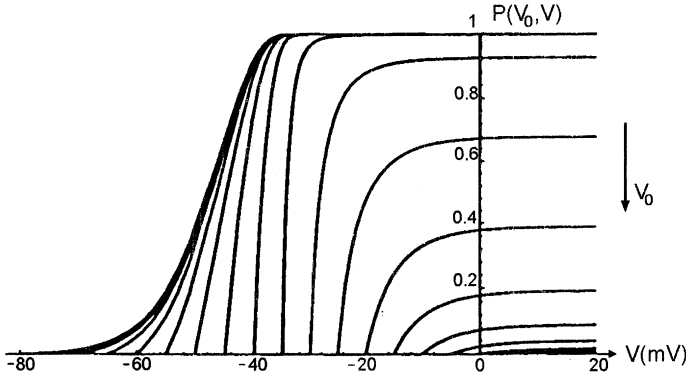

Fig. 2. Firing probabilities $P(V_0, V)$. Curves for different values of V_0 between -90 mV and $+5$ mV are shown. Note that firing occurs with probability close to 1 if $V_0 < \Theta$, but for higher starting potentials the firing probability becomes smaller until it vanishes around 0 mV. Most of the firing occurs around Θ, although some firing is also found at both lower and higher potentials

3 Behavior of the pyramidal cell model

Our goal was to reproduce the firing repertoire of the pyramidal cell as seen experimentally or as in more detailed models. The example we tried to follow is Traub's pioneering work (Traub and Miles 1991; Traub et al. 1991). Depending on the current injected into the soma, the two basic firing modes they describe is (1) low-frequency bursting, with the frequency increasing with the injected current; (2) repetitive firing, with the frequency increasing with the injected current.

The same repertoire has been found by Pinsky and Rinzel (1994) in a reduced model. Our aim is to demonstrate that our extremely reduced single-compartment model is still capable of reproducing these patterns.

First, the model without firing is analyzed to show that the difference between the two firing modes stems from interspike dynamics rather than from the firing properties of the cell. Then the bursting and repetitive firing patterns are reproduced by simulations with the complete model.

3.1 Analysis of interspike dynamics

In order to study the interspike behavior of the model, the firing probability function is set to zero. (This may correspond to the experimental situation where Na channels are blocked, e.g. by tetrodotoxin.) This reduces the model to two coupled ordinary differential equations: Eqs. (1) and (2). Systems like this can be investigated analytically as far as their long-term behavior is concerned. Software packages are also available for the bifurcation analysis. The results presented here have been made with the XPP package which uses the AUTO software (Doedel 1981) for the bifurcation analysis.

The external input current I_{ext} was chosen as the control parameter. The bifurcation diagram (Fig. 3A) shows that, for very small input currents, the membrane potential converges to a stable fixed point, i.e. the cell tends to return to its resting conditions. On increasing the current, a stable oscillation soon emerges with finite (nonzero) amplitude, and the fixed point loses stability. The involvement of calcium and the shape of the oscillations (Fig. 3C) show that repetitive *calcium spikes* are observed with long afterhyperpolarization (AHP) between the spikes. Nonzero amplitude at the bifurcation point demonstrates that the emergence of calcium spikes is an all-or-none phenomenon. The oscillation frequency (Fig. 3B) increases from 3.4 Hz to 22 Hz in the oscillatory regime. At still larger currents, the oscillation vanishes through a Hopf bifurcation, and the fixed point becomes stable again. This indicates that, without the firing mechanism, the cell would be silent for large currents.

In order to draw conclusions about the behavior of the full model with firing, it is important to observe the position of the fixed point as the input current is increased:

– If the input current is small, the fixed point is close to the resting potential, and thus *no firing* will occur.

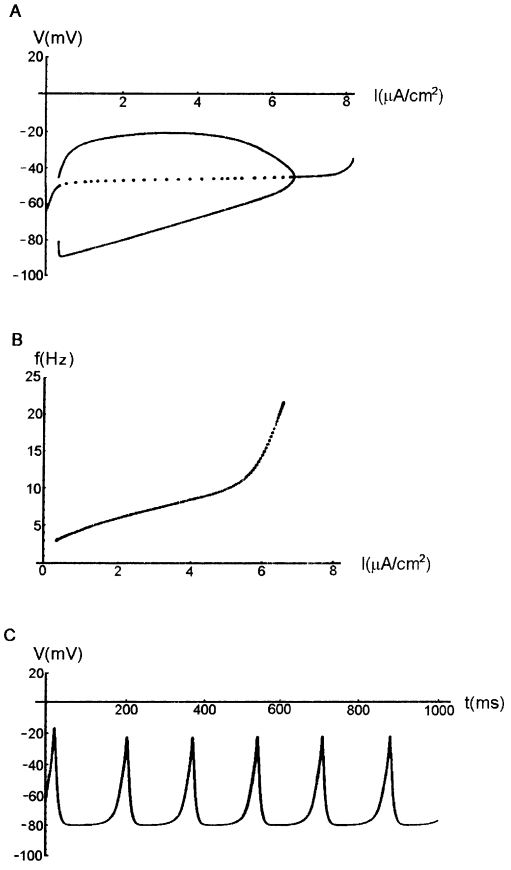

Fig. 3. A Bifurcation diagram of interspike dynamics. The constant external current was chosen as the bifurcation parameter. *Single solid line*: stable fixed point as a function of the control parameter. *Two solid lines*: oscillation minimum and maximum. *Dashed line*: unstable fixed point. Finite amplitude oscillation emerges at $I_{ext} = 0.356$ μA cm^{-2}, and it vanishes at a Hopf point at $I_{ext} = 6.624\,\mu$A cm^{-2}. **B** Frequency vs input current (*fI*) curve in the oscillation regime. **C** The time course of oscillation has similar characteristics to Ca spikes ($I_{ext} = 2\,\mu$A cm^{-2})

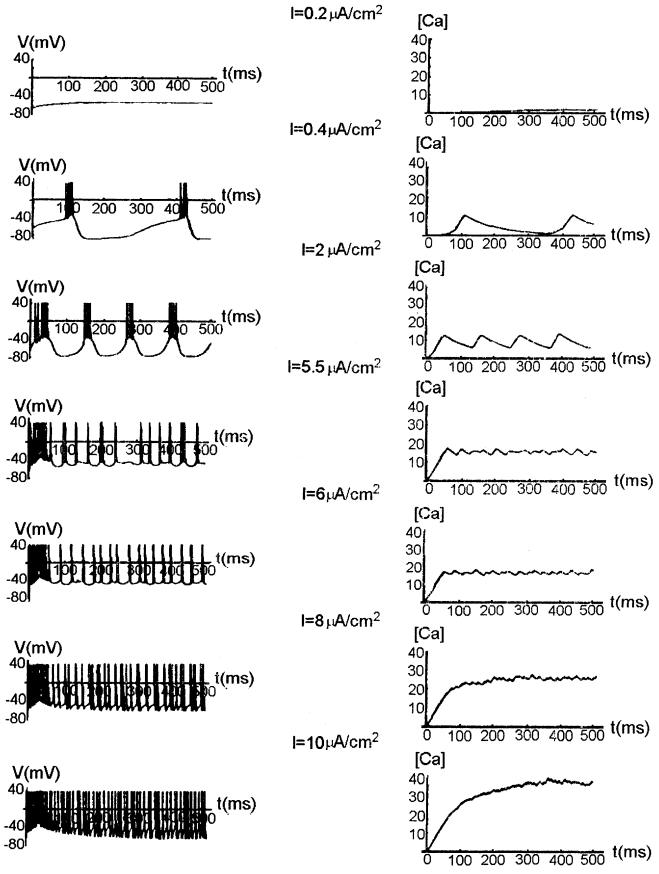

Fig. 4. Firing modes of the pyramidal cell model as the constant input current is varied. *Left*: membrane potential vs time. Spikes are visualized by a jump of the potential to 40 mV, followed by a linear decrease to the return value V_{ret}. *Right*: calcium concentration vs time. As the input current is increased, burst frequency becomes higher, and repetitive firing emerges around $I_{ext} = 6\,\mu$A cm^{-2} (cf. Traub et al. 1991; Figs. 4, 8; Traub and Miles 1991; Fig. 2.2)

– In the oscillatory regime, the unstable fixed point is between -50 mV and -45 mV: just where Na channels are about to open and firing is getting to have a high probability. Thus on the positive phase of the oscillations sodium spikes will appear, but not on the negative phase. This will lead to *bursting* behavior.
– At large currents, the fixed point is at a sufficiently depolarized membrane potential that the cell will fire, return to a membrane potential negative to the fixed point, and fire again, etc. In this way, *repetitive firing* will emerge.

3.2 Computer simulations

Simulations of the full model with firing were run to check the predictions of the bifurcation analysis. Figure 4 summarizes the results.

At small injected currents, no firing occurred, and both the membrane potential and calcium variables reached the fixed point predicted by the bifurcation analysis.

At currents larger than the first bifurcation point ($I_{ext} > 0.356$), bursts can be observed. The burst frequency (Fig. 5) agrees well with the values predicted by the bifurcation analysis (Fig. 3B). The burst shapes show similarity with those observed in experiments and in more detailed models.

If the input current is further increased, the number of spikes in a burst decreases, and doublets and single spikes appear. The larger the burst, the longer the following AHP lasts. This phenomenon was also found in detailed models (Traub and Miles 1991).

Passing the second bifurcation point ($I_{ext} > 6.624$), bursts and spike doublets completely disappear and repetitive firing emerges.

The burst frequency for small currents and the action potential frequency for larger currents are shown in Fig. 5. These *f-I* curves can be compared to those of Traub et al. (1991, Fig. 10) and of Pinsky and Rinzel (1994, Fig. 6). The burst frequency is higher in our model but the rate of repetitive firing is similar to their results. The firing frequency increases rapidly with the injected current.

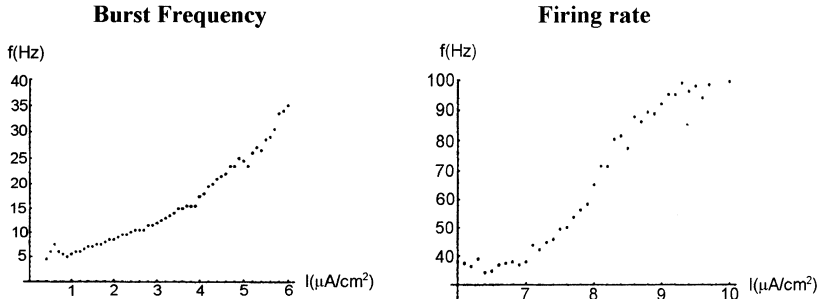

Fig. 5. *Left*: burst frequency as a function of input current. *Right*: frequency of repetitive firing vs input current (cf. Traub et al. 1991; Fig. 10)

4 Conclusions

A mathematical model has been presented to describe two cell types of the hippocampal CA3 region, pyramidal and inhibitory cells, and the synaptic interactions between them. This model is appropriate for the application as a single-cell module of the statistical population model to be presented in Part II.

The pyramidal cell model has been analyzed in detail. The model's main assumption was that, with a detailed description of interspike behavior, it is sufficient to add a very simple firing mechanism. Bifurcation analysis has supported this assumption, revealing that the important mechanisms underlying different firing modes are those involved in interspike dynamics. Computer simulations have shown that the basic firing reperoire of CA3 pyramidal cells can be reproduced by our model.

Appendix A. Pyramidal cells

A.1 Ionic currents

$$I_{Ca}(V) = \gamma_{Ca} \cdot s^5(V) \cdot (V - E_{Ca}) \tag{6}$$

$$I_K(V) = \gamma_K \cdot n^4(V) \cdot (V - E_K) \tag{7}$$

$$I_{K[Ca]}(V,X) = \gamma_{K[Ca]} \cdot q(V,X) \cdot (V - E_K) \tag{8}$$

$$I_L(V) = \gamma_L \cdot (V - E_{rest}) \tag{9}$$

where

$$s(V) = \frac{1}{1 + \exp((-45 - V)/10)} \tag{10}$$

$$n(V) = \frac{1}{1 + \exp((-40 - V)/15)} \tag{11}$$

$$q(V,X) = \frac{1}{1 + \exp((0.25V + 25 - X)/2)} \times \frac{1}{1 + \exp(2(2 - X))} \tag{12}$$

A.2 Parameter values

$$C = 1\ \mu\mathrm{F\,cm^{-2}} \tag{13}$$

$$\gamma_{Ca} = 0.1\ \mathrm{mS\,cm^{-2}} \tag{14}$$

$$\gamma_K = 0.15\ \mathrm{mS\,cm^{-2}} \tag{15}$$

$$\gamma_{K[Ca]} = 0.15\ \mathrm{mS\,cm^{-2}} \tag{16}$$

$$\gamma_L = 0.015\ \mathrm{mS\,cm^{-2}} \tag{17}$$

$$E_{Ca} = 75\ \mathrm{mV} \tag{18}$$

$$E_K = -95\ \mathrm{mV} \tag{19}$$

$$E_{rest} = -65\ \mathrm{mV} \tag{20}$$

$$B \cdot C = 0.5\ \mu\mathrm{M\,mV^{-1}} \tag{22}$$

A.3 Firing

To obtain a firing probability which fulfills the requirements of Sect. 2.3, we made the following considerations.

Obviously, for any V_0 ($V_0 < V_1 < V_2$),

$$P(V_0, V_2) = P(V_0, V_1) + (1 - P(V_0, V_1)) \cdot P(V_1, V_2) \tag{23}$$

that is

$$P(V_1, V_2) = \frac{P(V_0, V_2) - P(V_0, V_1)}{1 - P(V_0, V_1)} \tag{24}$$

Now let

$$P_0(V) = P(V_0, V) \tag{25}$$

Then

$$P(V_1, V_2) = \frac{P_0(V_2) - P_0(V_1)}{1 - P_0(V_1)} \tag{26}$$

Let us now define

$$p(V) = \lim_{\Delta V \to 0} \frac{P(V, V + \Delta V)}{\Delta V} \tag{27}$$

Then

$$p(V) = \lim_{\Delta V \to 0} \frac{P_0(V + \Delta V) - P_0(V)}{\Delta V} \cdot \frac{1}{1 - P_0(V)} = \frac{1}{1 - P_0(V)} \cdot \frac{dP_0(V)}{dV} \tag{28}$$

The solution of this differential equation is

$$P_0(V) = 1 - \exp\left(-\int_{V_0}^{V} p(v)dv\right) \tag{29}$$

and also

$$P(V_1, V_2) = 1 - \exp\left(-\int_{V_1}^{V_2} p(v)dv\right) \tag{30}$$

It is obvious that $P(V_1, V_2)$ is an increasing function of V_2 and it is easy to see (Requirement 3) that (if $V_1 < \Theta$) P should increase rapidly with V_2 before Θ and then saturate at nearly 1.

Now we show that it is unfavorable if $P_0(\infty) = 1$. This would mean that $\int_{V_0}^{\infty} p(v)dv = \infty$. If this integral was already infinite until Θ ($P_0(\Theta) = 1$) the cell would have to fire before Θ if $V_0 < \Theta$. This is not really what we want (e.g. because this would cause an instability when the return potential is around Θ). If, on the other hand,

the integral was finite until Θ, then it should be infinite after Θ and the cell would fire even if started from a large potential.

Thus for any V_0 the integral of p should be large until Θ ($1 \ll \int_{V_0}^{\Theta} p(v)dv < \infty$) but finite until infinity, i.e. $p(V)$ should tend to zero in the infinite limit.

For the simulations the following function was chosen:

$$p(V) = \begin{cases} q \cdot \exp((V-\Theta)/V^*) & \text{if } V < \Theta \\ q \cdot \exp(-(V-\Theta)/V^*) & \text{if } V \geq \Theta \end{cases} \tag{31}$$

$$\Theta = -35 \text{ mV} \tag{32}$$

$$V^* = 6 \text{ mV} \tag{33}$$

$$q = 1 \text{ mV}^{-1} \tag{34}$$

which yields $P(E_{\text{rest}}, \Theta) = 0.997$ and $P(E_{\text{rest}}, \infty) = 0.99999$.

When the firing probability $P(V_1, V_2)$ is determined, V_2 is calculated as if a sodium current $I_{\text{Na}}(V)$ also contributed to the change of the membrane potential. This current is described as

$$I_{\text{Na}}(V) = \gamma_{\text{Na}} \cdot m^3(V) \cdot h(V) \cdot (V - E_{\text{Na}}) \tag{35}$$

$$m(V) = \frac{1}{1 + \exp((-45 - V)/4)} \tag{36}$$

$$h(V) = \frac{1}{1 + \exp((30 + V)/4)} \tag{37}$$

$$\gamma_{\text{Na}} = 0.03 \text{ mS cm}^{-2} \tag{38}$$

$$E_{\text{Na}} = 50 \text{ mV} \tag{39}$$

The duration of the refractory state is

$$t^{\text{ref}} = 5 \text{ ms} \tag{40}$$

The amount of calcium entering the cell during firing is

$$X_{\text{ret}} - X = 1.5\,\mu M \tag{41}$$

and the restored membrane potential is

$$V_{\text{ret}}(X_{\text{ret}}) = \begin{cases} -55 + X_{\text{ret}}/(B \cdot C) & \text{if } X_{\text{ret}} < 10 \\ -30 - X_{\text{ret}} & \text{otherwise} \end{cases} \tag{42}$$

Appendix B. Inhibitory cells

B.1 Parameter values

$$\gamma_{\text{L}} = 0.03 \text{ mS cm}^{-2} \tag{43}$$

$$E_{\text{rest}} = -65 \text{ mV} \tag{44}$$

B.2 Firing
Firing threshold:

$$\Theta = -45 \text{ mV} \tag{45}$$

Acknowledgements. This work was supported by OTKA grants F014020 and T017784, by the exchange program between the Hungarian Academy of Sciences and the Consiglio Nazionale delle Ricerche (Italy), and by the Fogarty International Research Collaboration Award, HHS Grant No. 1 R03 TW00485-01.

References

Amari S (1974) A method of statistical neurodynamics. Kybernetik 14:201–25

Arbib MA, Érdi P, Szentágothai J (1997) Neural organization: structure, function, dynamics. MIT Press, Cambridge, Mass

Beurle RL (1956) Properties of a mass of cells capable of regenerating pulses. Phil Trans R Soc Lond 204A:55–94

Bower J, Beeman D (1995) The book of GENESIS. TELOS, The Electronic Library of Science, Springer, Berlin Heidelberg New York

Cartling B (1995) A generalized neuronal activation function derived from ion-channel characteristics. Netw Compat Neur Syst 6:389–401

Clark J, Rafelski J, Winston J (1985) Brain without mind: computer simulation of neural networks with modifiable neuronal interactions. Phys Rep 123:215–273

Doedel EJ (1981) AUTO: a program for the automatic bifurcation and analysis of autonomous systems. Cong Num 30:265–284

Érdi P, Aradi I, Grőbler T (1997) Rhythmogenesis in single cell and population models: olfactory bulb and hippocampus. BioSystems, 40:45–53

Ermentrout G (1995) Phase-plane analysis of neural activity. In: Arbib M (eds) The handbook of brain theory and neural networks, MIT Press, Cambridge, Mass., pp 732–738

FitzHugh R (1961) Impulses and physiological states in models of nerve membrane. Biophys. J., 1:445–466

Freund T, Buzsáki G (1996) Interneurons of the hippocampus. Hippocampus, 6:347–470

Griffith JA (1963) A field theory of neural nets. I. Derivation of field equations. Bull. Math. Biophys., 25:111–120

Grőbler T, Barna G (1996) A statistical model of the CA3 region of the hippocampus. In: Trappl R (eds) Cybernetics and systems '96. Austrian Society for Cybernetic Studies, Vienna, 1996 pp 503–507

Grőbler T, Barna G (1997) Single cell and population activity in a statistical model of the hippocampal CA3 region. In: Bower JM (edr) Computational Neuroscience (CNS 96). Plenum New York, pp 327–331

Hindmarsh JL, Rose RM (1982) A model of the nerve impulse using two first-order differential equations. Nature, 296:162–164

Hindmarsh JL, Rose RM (1984) A model of neuronal bursting using three coupled first-order differential equations. Proc R Soc Lond 221:87–102

Hines M (1984) Efficient computation of branched nerve equations. J. Bio-Med. Comput 15:69–74

Hines M (1993) The NEURON simulation program. In: Skrzypekr J (eds) Neural network simulation environments. Kluwer, Norwell, Mass.

Hodgkin A, Huxley A (1952) A quantitative description of membrane current and its application to conduction and excitation in nerve. J Physiol (Lond), 117:500–544

Horn D, Usher M (1989) Neural networks with dynamical thresholds. Phys Rev A 40:1036–1044

Ingber L (1982) Statistical mechanics of neocortical interactions. I. Basic formulation. Physica, 5D:83–107

Kepler T, Abbott L, Marder E (1992) Reduction of conductance-based neuron models. Biol Cybern 66:381–387

Lisman J (1997) Bursts as a unit of neural information: making unreliable synapses reliable. Trends Neurosci 20:38–43

Nagumo JS, Arimoto S, Yoshizawa S (1962) An active pulse transmission line simulating nerve axon. Proc IRE 50:2061–2070

Peretto P (1984) Collective properties of neural networks: a statistical approach. Biol Cybern 50:51–62

Peretto P (1992) An introduction to the modeling of neural networks. Cambridge University Press, Cambridge

Pinsky PF, Rinzel J (1994) Intrinsic and network rhythmogenesis in a reduced Traub model for CA3 neurons. J Comput Neurosci 1:39–60

Rinzel J (1987) A formal classification of bursting mechanisms in excitable systems. In: Teramoto E, Yamaguti M (eds) Lecture notes in Biomathematics 71: mathematical topics in population biology, morphogenesis, and neurosciences. Springer, Berlin Heidelberg New York, pp 267–281

Seelen W von (1968) Informationsverarbeitung in homogenen Netzen von Neuronenmodellen. Kybernetik 5:181–194

Traub RD, Miles R (1991) Neuronal networks of the hippocampus. Cambridge University Press, New York

Traub RD, Wong RKS, Miles R, Michelson H (1991) A model of a CA3 hippocampal pyramidal neuron incorporating voltage-clamp data on intrinsic conductances. J Neurophysiol, 66:635–650

Traub RD, Miles R, Muller R, Gulyás A (1992) Functional organization of the hippocampal CA3 region: implications for epilepsy, brain waves and spatial behaviour. Network, 3:465–488

Ventriglia F (1974) Kinetic approach to neural systems. I. Bull Math Biol 36:534–544

Ventriglia F (1988) Computational simulation of activity of cortical-like neural systems. Bull Math Biol 50:143–185

Ventriglia F (1994) Towards a kinetic theory of cortical-like neural fields. In: Ventriglia F (eds) Neural modeling and neural networks. Pergamon Press, Oxford, pp 217–249

Wilson M, Bower J (1989) The simulation of large-scale neural networks. In: Koch C, Segev I, (eds) Methods in neural modeling: from synapses to networks, MIT Press, Cambridge, Mass., pp 291–334

Wilson HR, Cowan JD (1973) A mathematical theory of functional dynamics of cortical and thalamic nervous tissue. Kybernetik, 13:55–80

Wong RKS, Prince DA (1978) Participation of calcium spikes during intrinsic burst firing in hippocampal neurons. Brain Res 159:385–390